Desalination and Water Treatment
www.deswater.com
49 (2012) 81–94
November
1944-3994/1944-3986 © 2012 Desalination Publications. All rights reserved
doi: 10.1080/19443994.2012.708202
Taylor & Francis
Taylor & Francis Group

Prediction of optimum adsorption isotherm: comparison of chi-square and Log-likelihood statistics

Mahdi Hadi[a,b,*], Gordon McKay[c], Mohammad Reza Samarghandi[d], Afshin Maleki[a], Mehri Solaimany Aminabad[a]

[a]*Kurdistan Environmental Health Research Center, Faculty of Health, Kurdistan University of Medical Sciences, Sanandaj, Iran*
Tel. +98 9189061738; email: hadi_rfm@yahoo.com
[b]*Center for Water Quality Research (CWQR), Institute for Environmental Research (IER), Tehran University of Medical Sciences, Tehran, Iran*
[c]*Department of Chemical and Biomolecular Engineering, Hong Kong University of Science and Technology, Clearwater Bay, New Territory, Hong Kong SAR*
[d]*Department of Environmental Health Engineering, School of Public Health, Center for Health Research, Hamadan University of Medical Sciences, Hamadan, Iran*

Received 8 June 2011; Accepted 9 May 2012

ABSTRACT

A comparison of chi-square (X^2) and Log-likelihood (G^2) statistics of 19 adsorption isotherm models—seven two-parameter models (Langmuir, Freundlich, Dubinin–Radushkevich, Temkin, Jovanovic, Harkins–Jura and Halsey) and 12 three-parameter models (Koble–Corrigan, Langmuir–Freundlich, Tóth, Redlich–Peterson, Radke–Prausnitz (three models), Fritz–Schlunder, Jossens, Khan, UNILAN, Vieth–Sladek) have been applied to the experiment of two dyes (Acid Blue 113, Acid Black 1) sorption onto Granular PineCone derived Activated Carbon (GPAC) and three dyes (Acid Blue 80, Acid Red 114, Acid Yellow 117) sorption onto Granular Activated Carbon type Filtrasorb 400 (GAC F400). The study has focused on the assessment of the adequacy and goodness of the fitted models, using two well-known—X^2 and G^2—statistics. The results showed that G^2 could be better than X^2 statistic when the number of model parameters is three.

Keywords: Adsorption; Isotherm models; Chi-square statistic; Log-likelihood statistic

1. Introduction

Adsorption phenomena have been known to mankind and increasingly utilized to perform desired bulk separation or purification purposes. The heart of an adsorption process is usually a porous solid medium. Porous solids provide a very high surface area or micropore volume thus high adsorptive capacity can be achieved. Adsorption equilibria information is the most important piece of information in understanding an adsorption process. The adsorption equilibria of pure components are essential to the understanding of how much those components can be accommodated by a solid adsorbent [1].

The equilibrium isotherm represents the distribution of the adsorbed material between the adsorbed phase and the solution phase at equilibrium. This isotherm is characteristic for a specific system at a particular thermal condition [2].

So far, several isotherm models with different assumptions have been developed to examine the

*Corresponding author.

adsorption mechanism. However, many models can not describe well the experimental data. To finding the best model among all models statistical methods are needed to find the best model.

The linear least-squares method with linearly transformed isotherm equations has been widely applied to confirm experimental data and isotherms using coefficients of determination [3]. However, transformations of nonlinear isotherm equations to linear forms can alter their error structure and may also violate the error variance and normality assumptions of standard least squares [4].

The linear equation analysis using the R^2 calculation associated with the sum of normalized errors (SNE) calculation procedure presented an appropriate method to use for the study of Ochratoxin A adsorption onto yeast by-products [5] but the nonlinear chi-square method provided better determination for the three sets of experimental data for the sorption isotherms of reactive dye from aqueous solutions by compost [6].

In recent years, several error analysis methods, such as the coefficient of determination, the sum of the errors squared, a hybrid error function, Marquardt's percent standard deviation, the average relative error, the sum of the absolute errors, chi-square, *F*-test and Students *t*-test have been used to determine the best-fitting isotherm equation [3,7–10].

It is not appropriate to use the correlation coefficient (R) or the coefficient of determination (R^2) of linear regression analysis for comparing the adsorption isotherms. Nonlinear chi-square (X^2) analysis could be a better method [8].

Nonlinear optimization provides a more complex and mathematically rigorous method for determining isotherm parameter values [11–13], but still requires a measure of the goodness-of-fit of an estimated statistical model in order to evaluate the fit of the isotherm models to the experimental data.

G-square (G^2) is another statistic to find the model that best explains the data. The *G*-square test for goodness-of-fit also known as log-likelihood statistic and is an alternative to the chi-square test of goodness-of-fit. The distribution of G^2 statistic under the null hypothesis is approximately same as the theoretical chi-square distribution. Thus, the probability of getting values of G and X can be calculated using the chi-square distribution [14,15].

In this study, the adsorption equilibrium isotherms of five dyes (Acid Blue 113, Acid Black 1, Acid Blue 80, Acid Red 114 and Acid Yellow 117), from aqueous solution onto activated carbon were studied and modeled. A trial-and-error nonlinear method of seven two-parameter isotherms—Langmuir [16], Freundlich [17], Dubinin–Radushkevich [18], Jovanovic [19], Harkins–Jura [20], Temkin [21], Halsey [22]—12 three-parameter models—Koble–Corrigan [23], Langmuir–Freundlich [24], Tóth [25], Redlich–Peterson [26], Fritz–Schlunder [27], Radke–Prausnitz (three models) [28], Jossens [29], Khan [30], UNILAN [31], Vieth–Sladek [32]—was used to determine the best fit isotherm. The G^2 and X^2 statistics were used in assessment of the adequacy and goodness-of-fitted models. The purpose of this study is to compare G^2 and X^2 statistics to find the best isotherm model. The values of probability to getting G and X for each model were calculated and compared.

2. Materials and methods

2.1. Facilities

Weighing of materials was performed by using an analytical balance with precision of ±0.0001 g (model Sartorius ED124S). Drying of materials was carried out in an electric oven (model PARS TEB) and carbonization in a muffle furnace (model Exiton). The pH of solutions was measured using a digital pH-meter (model Sartorius Professional Meter PP-50). The dye solutions were stirred using an inductive stirring system (Oxitop IS 12) within a WTW-TS 606/2-i incubator. The samples were centrifuged using a 301 Sigma Centrifuge. The dye concentration in the samples was measured spectrophotometrically, using a UV-1,700 Pharmaspec Shimadzo spectrophotometer.

2.2. Raw materials

Dried pinecone was used as the raw material to produce the adsorbent. The pinecones were collected from the Mardom Park in front of Hamadan University of Medical Sciences of Iran. The ground pinecone derived activated carbon (GPAC) is advantageous over carbons made from other materials because of its high density and high purity. This carbon is harder and more resistant to attrition [33,34]. Acid Blue 113 (AB113) one disazo type dye and Acid Black 1 (AB1), a sulfonated azo dye were used in this study. AB113 and AB1 dyes were obtained from Alvansabet dyestuff and textile auxiliary manufacturer company in the west of Iran.

The experiments for three other dyes, namely Acid Blue 80 (AB80), Acid Red 114 (AR114) and Acid Yellow 117 (AY117) were conducted by Choy et al. [35]. Their experimental data were provided by Prof. Gordon McKay and used in this study. The dyestuffs were used as the commercial salts. The AB80 and AY117 were supplied by Ciba Speciality Chemicals

Table 1
Information regarding the acid dyes

Name of dyes	AB1	AB113	AB80	AR114	AY117
Color index number	20470	26360	61585	23635	24820
Molecular mass (g)	618	681	676	830	848
λ_{max} (nm)	622	574	626	522	438

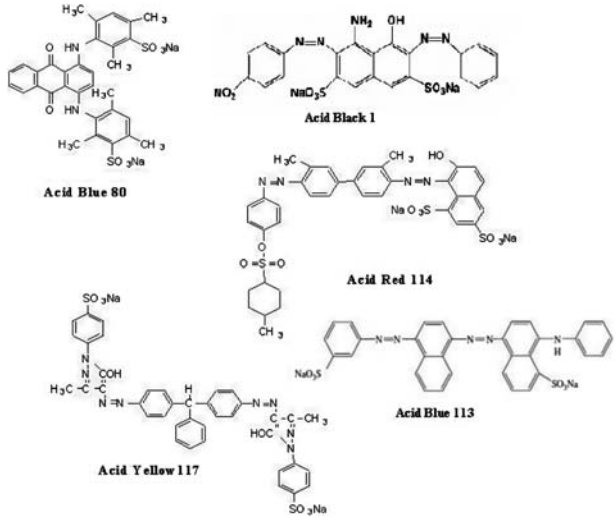

Fig. 1. Dye structures of AR114, AB80, AY117, AB1, and AB113.

and AR114 was supplied by Sigma–Aldrich chemical company.

Some information regarding the five acid dyes, which were used to measure and prepare standard concentration dye solutions, is listed in Table 1. The data include color index number, molecular mass and the wavelengths at which maximum absorption of light occurs, λ_{max}. The structures of the five acid dyes are shown in Fig. 1 and information regarding them is listed in Table 1.

2.3. Adsorbents

2.3.1. Pinecone derived activated carbon

The local granular activated carbon was produced by exposing the raw pinecones to a thermal–chemical process. The pinecones were crushed and washed with hot water and then dried at 100˚C in an oven overnight. A 50-g crushed sample was mixed with a pre-determined volume of phosphoric acid with concentration of 95% in the mass ratio of 1:10. This mixture was transferred to a stainless steel tube (50 mm diameter and 250 mm long). This tube was placed on a tile as insulator and inserted into a muffle furnace which was programmed to gradually reach up to 900˚ C within 3 h, this temperature was maintained for 1 h, and then gradually cooled down to the room temperature. The end product was repeatedly washed using hot distilled water until the washings showed pH >6.9; the washed sample was then again dried at 120˚ C in an oven overnight. The final sample was then ground in a household-type blender and passed through a series of sieves (20, 30, 40, 50 US standard mesh sizes). A mixture of the residuals on 30, 40, and 50 sieves was kept in an air-tight bottle and used as the adsorbent in this study. The average adsorbent particle size was 0.5 mm.

The specific surface area of local GPAC was obtained by the determination of the optimal concentration of methylene blue dye adsorbed onto the GPAC sorbent at constant temperature 20˚C. The methylene blue calculated surface area was $734\,m^2\,g^{-1}$.

The potential capacity of an adsorbent for adsorption can be evaluated through iodine adsorption from aqueous solutions using test conditions referred to as the iodine number determination. The iodine number was measured according to the standard procedure [36]. The calculated Iodine Number value was $483.5\,mg\,g^{-1}$. The apparent density was calculated by filling a calibrated cylinder with a given activated carbon weight and tapping the cylinder until a minimum volume was recorded. This density was referred as tapping or bulk density of adsorbent. For the real density a pycnometer method was used, which consisted of filling a pycnometer with the activated carbon, then added a solvent (methanol) to fill the void, at each step the weight was determined. The apparent and real density values were equal to 0.50 and $1.70\,g\,cm^{-3}$, respectively. The pore volume and the porosity were determined by using a volumetric method which consists of filling a calibrated cylinder with a V_1 volume of activated carbon (mass m_1) and solvent (methanol) until volume V_2 (total mass m_2) is reached. Knowing the density of solvent, total porosity volume ($1.40\,cm^3\,g^{-1}$) and the porosity (70%) of the adsorbent were easily calculated. The BET nitrogen surface area was determined to be $869\,m^2\,g^{-1}$.

2.3.2. Activated carbon F400

The other adsorbent used in the research (conducted by Choy et al. [35]) was a Granular Activated Carbon type F400 (GAC F400); it was supplied by Chemviron Carbon Ltd.

GAC F400 was crushed by using a hammer mill and washed with distilled water to remove fines. It was dried at 110°C in an oven for 24 h and then sieved. The 500–710 μm size range activated carbon was used for the experiments [35]. The BET nitrogen surface area was reported by the supplier to be $1150\,m^2\,g^{-1}$.

2.4. Adsorption data

Accurately weighed quantities of AB113 and AB1 dyes were dissolved in distilled water to prepare stock solutions ($500\,mg\,L^{-1}$). The calibration curves for AB113 and AB1 were linear from 0.125 to $100\,mg\,L^{-1}$ ($R^2 = 0.999$) and 0.062 to $100\,mg\,L^{-1}$ ($R^2 = 0.999$), respectively. The synthetic dyes solutions were prepared by diluting stock solutions to produce solutions of $150\,mg\,L^{-1}$ of each dye. The adsorption equilibrium experiments were carried out in a batch process in 250-mL Erlenmeyer flasks housed in an incubator container. To determine the equilibrium time of AB113 and AB1 adsorption onto GPAC, an accurate amount of 0.12 g of GPAC with 250 mL of each dye solution ($150\,mg\,L^{-1}$) was added to two Erlenmeyer flasks. The contents of flasks were mixed using a magnetic stirrer and 1 mL samples were taken at regular times. The dye concentration in the samples was measured spectrophotometrically after centrifugation at 3800 rpm for 5 min. The equilibrium times for AB113 and AB1 were determined to be 250 and 167 h, respectively. To perform isotherm experiments, accurately weighed amounts of GPAC adsorbent of 0.01, 0.02, 0.04, 0.06, 0.08, 0.1, 0.12, 0.14, 0.16, 0.18, and 0.2 g for AB 113 and AB1 were added to several flasks with 250 mL dye solution ($150\,mg\,L^{-1}$) at pH 7.4 ± 0.2 for AB113 and 7.0 ± 0.2 for AB1 dyes. The pH values at the end of batch runs were 6.1 ± 0.2 and 5.9 ± 0.2 for AB113 and AB1 dyes, respectively. The content of all Erlenmeyer flasks were mixed thoroughly for 250 and 167 h for AB113 and AB1 respectively at 20.3°C using magnetic stirrers at constant revolution. A 5-ml sample was taken after the equilibrium time and centrifuged at 3,800 rpm for 5 min. the residual dye concentration was measured spectrophotometrically.

The $250\,mg\,L^{-1}$ concentration dye solutions for AB80, AR114, and AY117 dyes were used to determine the equilibrium contact time. For each acid dye system, eight jars of fixed volume (0.05 L) of dye solutions were prepared and contacted with 0.05 g activated carbon F400 (GAC F400). Then, the jars were put into the shaking bath with the same conditions of the isotherm adsorption experiment (constant temperature 20°C and 200 rpm shaking rate). At 3-day intervals, one of the jars was taken from the shaker and the dye concentration was measured. By plotting the acid dye adsorption capacity of the activated carbon against the time, it was found that the activated carbon adsorption capacity became constant after a certain period of time. It implied that the dye adsorption system had reached equilibrium at that time. Therefore, the equilibrium contact time can be determined from the graph. The activated carbon adsorption capacity of all three acid dyes (AB80, AR114 and AY117) in the samples became constant after 21 days. The equilibrium contact time for the sorption equilibrium studies has been shown to be 21 days minimum [35].

The amount of dye adsorbed onto the sorbent, was calculated as follows:

$$q_e = \frac{(C_0 - C_e)V}{m} \tag{1}$$

Each isotherm study was repeated three times and the mean values have been reported.

2.5. Assessing goodness-of-fit by G^2 and X^2

The Pearson chi-square (X^2) and log-likelihood (G^2) statistics are two well-known statistics for assessing the goodness-of-fit of a regression model. These statistics can be used to test that the observed data came from an experiment in which the fitted model is true. They are based on observed and expected observations [37].

2.5.1. Chi-square statistic

The advantage of using chi-square test is for comparing all isotherms on the same abscissa and ordinate [8]. The chi-square test statistic is basically the sum of the squares of the differences between the experimental data obtained by calculating from models with each squared difference divided by the corresponding data obtained by calculating from models. The equivalent mathematical statement is:

$$X^2 = \sum_{i=1}^{N} \frac{(q_{exp,i} - q_{m,i})^2}{q_{m,i}} \tag{2}$$

where $q_{exp,i}$ and $q_{m,i}$ are the equilibrium capacity ($mg\,g^{-1}$) obtained from the experiment and model, respectively. Here, the values q_{exp} are called the observed values and the modeled values q_m are sometimes called the predicted values. N is sample size or number of experimental data points. The chi-square statistic can be used to calculate a p-value

by comparing the value of the statistic to a chi-square distribution. The number of degrees of freedom is equal to the number of experimental data points (N), minus the number of model parameters [14].

2.5.2. G-square statistic

The G-square test statistic is calculated by taking an observed number (q_{exp}), dividing it by the predicted number (q_m), then taking the natural logarithm of this ratio. The test statistic is usually called G^2, and thus this is a G^2-test, although it is also sometimes called a log-likelihood test or a likelihood ratio test. The equation is:

$$G^2 = 2\sum_{i}^{N}\left[q_{exp,i} \times \ln\left(\frac{q_{exp,i}}{q_{m,i}}\right)\right] \quad (3)$$

As with most test statistics, the larger the difference between observed and expected, the larger the test statistic becomes. Once the G-statistic known; the probability of getting that value of G can be calculated using the chi-square distribution. The shape of the chi-square distribution depends on the number of degrees of freedom. The number of degrees of freedom is simply the number of experimental data points (N), minus the number of model parameters [14,37].

2.6. Adsorption models

Nineteen different isotherm models were used for describing the single-component experimental isotherm data. The names and the nonlinear forms of studied isotherm models are shown in Table 2. Fitting of the adsorption isotherm models to the experimental data is performed using OriginPro (Version 8.0) Software. In this study, the values of standard error after model convergence by an iteration process were satisfied because each model converged acceptably until the reduced chi-square received the minimum.

To find the optimum model, G^2 and X^2 statistics were calculated for all models and the models were sorted by X^2 and G^2 from the smallest to the largest.

3. Results and discussion

The calculated isotherm parameters of two-parameter and three-parameter isotherm models and their corresponding X^2 and G^2 statistics are shown in Tables 3 and 4, respectively.

Several authors have introduced the comparison of different error functions. The applicability of linear or nonlinear isotherm models has been examined in describing the adsorption of dyes, heavy metals, and organic pollutants onto a list of low-cost adsorbents (Table 5). Linear regression analysis has frequently been employed in assessing the quality of fits [38] and adsorption performance. However, during the last few

Table 2
The name and nonlinear form of studied isotherm models

Parameters number	Isotherm	Non-linear form	Isotherm	Non-linear form
2	Langmuir	$q_e = \frac{q_m b C_e}{1+bC_e}$	Harkins-Jura	$q_e = \left(\frac{A_H}{B_H - \log C_e}\right)^{1/2}$
	Freundlich	$q_e = k_f C_e^{1/n}$	Halsey	$q_e = \mathrm{Exp}\left(\frac{\ln k_H - \ln C_e}{n}\right)$
	Dubinin–Radushkevich	$q_e = Q_s \mathrm{Exp}(-B_D\varepsilon^2)$, $\varepsilon = RT\ln\left(1+\frac{1}{C_e}\right)$	Temkin	$q_e = \frac{RT}{b_T}\ln(K_{T_e}C_e)$
	Jovanovic	$q_e = q_{max}(1 - e^{(k_j C_e)})$		
3	Jossens	$q_e = \frac{k_j C_e}{1+jC_e^{\beta}}$	Koble–Corrigan	$q_e = \frac{A_C C_e^{\beta}}{1+B_C C_e^{\beta}}$
	Khan	$q_e = \frac{q_{mk} b_k C_e}{(1+b_k C_e)^{\beta}}$	Redlich-Peterson	$q_e = \frac{A_R C_e}{1+B_R C_e^{\beta}}$
	Tóth	$q_e = \frac{q_{mT} C_e}{\left(1/K_T + C_e^{m_T}\right)^{1/m_T}}$	Vieth-Sladek	$q_e = \left(\frac{S_{max} k_L C_e}{1+k_L C_e}\right) + k_d C_e$
	Radke I	$q_e = \frac{q_{mRP} K_{RP} C_e}{(1+K_{RP}C_e)^{m_{RP}}}$	Fritz	$q_e = \frac{q_{mFS} K_{FS} C_e}{1+k_{FS} C_e^{m_{FS}}}$
	Radke II	$q_e = \frac{q_{mRP} K_{RP} C_e}{1+K_{RP} C_e^{m_{RP}}}$	UNILAN	$q_e = \frac{q_{mu}}{2s}\ln\left(\frac{1+K_u C_e e^{s}}{1+K_u C_e e^{-s}}\right)$
	Radke III	$q_e = \frac{q_{mRP} K_{RP} C_e^{m_{RP}}}{1+K_{RP} C_e^{m_{RP}-1}}$		
	Langmuir–Freundlich	$q_e = \frac{q_{mLF}(K_{LF}C_e)^{m_{LF}}}{1+(K_{LF}C_e)^{m_{LF}}}$		

Table 3
Isotherm parameters, X^2 and G^2 statistics of two-parameter models

Model	Parameter	AB113	AB1	AB80	AR114	AY117
Jovanivic	G^2	17.427	135.870	30.752	22.067	55.201
	X^2	6.409	48.711	7.533	6.650	16.047
	q_{max}	271.3	433.6	152.4	92.2	167.0
	k_j	0.081	0.492	0.120	0.114	0.166
Temkin	G^2	1.991	18.945	3.227	1.038	2.419
	X^2	1.986	19.251	3.113	**1.016**	**2.380**
	k_{Te}	6.892	126.8	2.029	1.993	3.507
	b_T	57.368	49.306	75.710	125.404	73.543
Harkins–Jura	G^2	1550.043	1423.123	914.523	634.621	951.459
	X^2	266.718	292.791	317.472	205.820	336.762
	A_H	177559.4	544231.1	27557.5	9856.8	31221.4
	B_H	6.970	7.196	5.477	5.399	5.144
Dubinin–Radushkevich	G^2	13.125	83.195	213.330	101.241	348.305
	X^2	9.839	57.883	635.807	184.519	9378.343
	Q_s	269.4	417.4	145.3	88.51	158.3
	B_D	0.028	0.001	0.006	0.007	0.003
Freundlich	G^2	1.920	20.522	8.672	2.627	5.340
	X^2	3.406	32.132	21.937	7.963	20.831
	k_f	124.1	253.4	46.90	28.06	56.48
	n	5.740	7.570	3.475	3.445	3.534
Halsey	G^2	1.902	20.419	8.592	2.585	5.247
	X^2	3.406	32.137	21.947	7.966	20.843
	k_H	0.000	0.000	0.000	0.000	0.000
	n	−5.741	−7.572	−3.476	-3.446	−3.536
Langmuir	G^2	1.904	26.370	1.070	3.984	12.544
	X^2	**0.836**	**8.907**	**1.116**	1.329	2.476
	q_m	298.4	452.8	171.4	103.7	185.8
	b	0.124	0.788	0.150	0.144	0.216

years, a development interest in the utilization of nonlinear optimization modeling has been noted [5].

As Table 5 shows, the G^2 is one function that has been rarely used in literatures. Ho [8] examined that nonlinear chi-square (X^2) analysis could be a better method for comparing the best fitting of isotherm models. The applicability of five statistical tools to satisfactorily determine the best-fitting isotherm model for both linear and nonlinear analysis was also investigated by Ncibi [6]. He showed that the X^2 and Student's t-tests could be useful, with R^2, in the case of linear analysis. The R, R^2, X^2, and F-test seem to be adequate to point out the best-fitting isotherm model after a nonlinear regression approach. On the other hand, nonlinear approaches for avoiding the errors will impact the final determination. In this study, we compared G^2 and X^2 statistics to finding the best-fitted isotherm models using nonlinear regression.

To decide what statistic could be better to compare the isotherm models; each statistic p-value was determined using S-Plus software and the p-values difference of the two successive models sorted by X^2 were compared with that sorted by G^2 (Mann-Whitney U test was used).

The concept of the null hypothesis in goodness-of-fit test is: "The model is adequate"; therefore; the large value of calculated p-value is an evidence for accepting the model [37]. Thus, it can be inferred that if the p-values difference of two successive sorted models regarding the first statistic (G^2) be more than that of the second (X^2), the first would be the more sensitive statistic to finding the best model.

The sorted isotherm models by X^2 and G^2 statistics from smallest to largest and the corresponding p-value differences are shown in Tables 6 and 7, respectively. For instance, as shown in the first column of Table 6, the difference between the p-values for Langmuir and Temkin models is $3.48E{-}03$ and for Temkin and Freundlich is $2.62E{-}02$. The corresponding p-values for G^2 statistic regarding the

Table 4
Isotherm parameters, X^2 and G^2 statistics of three-parameter models

Model	Parameter	AB113	AB1	AB80	AR114	AY117
Tóth	G^2	0.696	6.495	1.993	0.739	0.426
	X^2	0.597	3.790	1.251	1.167	0.984
	m_T	0.777	0.707	0.887	0.668	0.718
	q_{mT}	314.0	472.9	177.2	119.3	205.5
	K_T	0.271	1.312	0.203	0.359	0.426
Jossens	G^2	1.011	11.819	2.376	1.247	0.415
	X^2	0.639	5.402	1.157	0.912	0.857
	j	0.177	1.113	0.193	0.312	0.388
	K_j	44.2	440.8	28.3	20.6	51.9
	β	0.965	0.968	0.965	0.899	0.921
Redlich–Peterson	G^2	0.797	11.863	2.313	1.220	0.406
	X^2	0.639	5.401	1.156	0.912	0.857
	B_R	0.177	1.113	0.193	0.312	0.388
	A_R	44.2	440.9	28.3	20.6	51.9
	β	0.965	0.968	0.965	0.899	0.921
Langmuir–Freundlich	G^2	0.678	5.980	**1.521**	**0.567**	0.790
	X^2	0.588	3.481	1.300	1.322	1.113
	q_{mLF}	312.2	470.4	174.9	113.8	198.9
	K_{LF}	0.123	0.776	0.142	0.110	0.178
	m_{LF}	0.819	0.761	0.944	0.797	0.828
Koble–Corrigan	G^2	0.658	5.931	1.548	**0.551**	0.776
	X^2	0.588	3.480	1.298	1.319	1.112
	A_C	56.3	387.7	27.7	19.6	47.7
	B_C	0.180	0.824	0.159	0.173	0.240
	β	0.819	0.761	0.944	0.797	0.828
Khan	G^2	0.911	12.653	2.364	1.248	1.024
	X^2	0.648	5.667	1.112	0.813	0.853
	q_{mk}	262.1	391.3	149.3	68.6	135.4
	b_k	0.162	1.079	0.186	0.280	0.362
	β	0.960	0.967	0.953	0.875	0.904
UNILAN	G^2	**0.649**	**4.331**	1.893	0.647	**0.257**
	X^2	0.575	3.138	1.271	1.222	1.020
	s	1.644	2.037	0.967	1.989	1.709
	q_{mu}	306.8	463.4	174.9	114.2	197.3
	K_u	0.130	0.811	0.142	0.109	0.182
Vieth–Sladek	G^2	1.172	19.302	1.922	1.476	2.713
	X^2	0.703	7.227	1.048	0.584	0.907
	S_{max}	287.4	437.1	162.1	86.8	163.9
	k_L	0.138	0.872	0.167	0.206	0.279
	k_d	0.082	0.189	0.104	0.195	0.328
Fritz–Schlunder	G^2	0.879	11.781	2.365	1.272	0.444
	X^2	0.639	5.399	1.156	0.912	0.857
	q_{mFS}	250.7	396.1	146.8	66.2	134.1
	K_{FS}	0.177	1.113	0.193	0.312	0.388
	m_{FS}	0.965	0.968	0.965	0.899	0.921
Radke I	G^2	0.890	12.6	2.305	1.287	0.991
	X^2	0.648	5.665	1.112	0.813	0.853
	q_{mRP}	262.1	391.2	149.3	68.6	135.3

(*Continued*)

Table 4 (*continued*)

Model	Parameter	AB113	AB1	AB80	AR114	AY117
	k_{RP}	0.162	1.080	0.186	0.280	0.362
	m_{RP}	0.960	0.967	0.953	0.875	0.904
Radke II	G^2	0.887	11.7	2.314	1.271	0.445
	X^2	0.639	5.398	1.156	0.912	0.857
	q_{mRP}	250.7	396.1	146.8	66.2	134.1
	k_{RP}	0.177	1.114	0.193	0.312	0.388
	m_{RP}	0.965	0.968	0.965	0.899	0.921
Radke III	G^2	0.802	11.8	2.314	1.245	0.403
	X^2	0.639	5.404	1.157	0.914	0.857
	q_{mRP}	44.2	440.6	28.3	20.7	52.0
	k_{RP}	5.667	0.899	5.182	3.197	2.579
	m_{RP}	0.035	0.032	0.035	0.102	0.079

isotherm models are shown in Table 7. The difference between the *p*-values for Halsay and Langmuir models is $1.11E{-}05$ and for Langmuir and Freundlich is $1.04E{-}04$. The *p*-values difference values within each column of Table 6 compared with corresponding values in Table 7.

The differences of X^2 *p*-values (difference between *p*-values of two best successive three parameter models) for sorted three-parameter models (Table 6) was compared with corresponding values in Table 7 (difference between G^2 *p*-values of two best successive three parameters models). The Mann–Whitney U test was used for the comparison, and it was found at 0.05 level the two distributions are significantly different (*p*-value = 0.00323). The results of Mann–Whitney U test are shown in Table 8. Moreover, the value of the mean rank for X^2 *p*-value difference distribution was less than that for G^2 ($46.6 < 64.4$). These results show the sensitivity of G^2 statistic is more than that for X^2 in finding the best three-parameter model regarding goodness-of-fit. Therefore, the G^2 statistic is found to be more appropriate than X^2 for comparing the models with three parameters. In other words, the sensitivity of G^2 statistic may be increased by increasing the number of model parameters in comparison with X^2.

The differences of X^2 *p*-values (difference between p-values of two best successive two-parameter models) for sorted two-parameter models were also shown in Table 6. These values were compared with corresponding values in Table 7 (differences of G^2 *p*-values of two best successive two-parameter models).

It was found at 0.05 level the two distributions are not significantly different (*p*-value = 0.79012) (Table 8). Therefore, the G^2 and X^2 may have similar sensitivity for the comparison of two-parameter models. However, because the mean rank for X^2 statistic is more than that for G^2 ($31.1 > 29.8$) (Table 8), the X^2 statistic may be better to be used instead of the G^2 statistic when the aim is finding the best among two-parameter models.

Based on our findings, the best two- and three-parameter isotherm models to describe the sorption of studied dyes were found as follows:

AB113: Langmuir (two-parameter), UNILAN (Three-parameters)
AB1: Langmuir (two-parameter), UNILAN (Three-parameters)
AB80: Langmuir (two-parameter), Langmuir-Freundlich (Three-parameters)
AR114: Temkin (two-parameter), Langmuir-Freundlich (Three-parameters)
AY117: Temkin (two-parameter), UNILAN (three-parameters)

The experimental isotherm data and best fitted models for the sorption of AB1 and AB113 dyes onto GPAC and AB80, AR114 and AY117 dyes onto GAC F400 are shown by Figs. 2 and 3 separately.

The two-parameter Langmuir and three-parameter UNILAN isotherm models were found statistically to be the best models to describe AB1 and AB113 dyes sorption onto GPAC. By comparison of their G^2 and X^2 statistics, it will be revealed that the UNILAN model describes adequately experimental sorption data. This is usually attributed to the complexity of the GPAC which is not as homogeneous as is assumed in Langmuir model. Thus to account for surface heterogeneity, an energy distribution can be introduced. In the UNILAN equation, a patch-wise surface is assumed. Each patch is assumed ideal such

Table 5
Previous researches of the linear and nonlinear isotherm studies

Adsorbent	Adsorbate	Isotherm models	Statistics	Model types	References
Activated carbon	Congo red	Freundlich, Langmuir, Redlich–Peterson	R^2	Nonlinear	[38]
Rice husk ash	Brilliant green dye	Freundlich, Langmuir, Redlich–Peterson, Temkin, Dubnin–Radushkevich	SSE, SAE, ARE, HYBRID, MPSD	Linear & Nonlinear	[39]
Activated carbon	Methylene blue	Freundlich, Langmuir, Redlich–Peterson	R2, ERRSQ, ARE, HYBRID, MPSD, EABS	Nonlinear	[40]
Rice husk	Methylene blue	Langmuir, Freundlich, Temkin Redlich-Peterson, Langmuir-Freundlich	R^2	Nonlinear	[41]
Chitosan	Congo red	Langmuir, Freundlich,Temkin, Koble–Corrigan, Toth	SSE, R^2	Nonlinear	[42]
Shaddock peel	Methylene blue	Freundlich, Langmuir,	R^2	Nonlinear	[43]
Laterite	Phosphorus	Langmuir, Freundlich, Redlich–Peterson	R^2	Linear & Nonlinear	[44]
Coal fly ash	Methyl orange	Freundlich, Langmuir, Redlich–Peterson (R–P), Dubnin–Radushkevich	SSE, SAE, ARE, HYBRID, MPSD	Linear & Nonlinear	[45]
Pinecone derived activated carbon	Methyl orange	Langmuir, Dubinin-Radushkevic, Temkin, Freundlich, Halsey, Harkins-Jura	RMSE, X^2	Nonlinear	[46]
Pinecone derived activated carbon & Activated carbon f400	Acid dyes	Langmuir, Freundlich, Dubinin–Radushkevich, Temkin, Halsey, Jovanovic , Harkins–Jura	G^2, X^2, RMSE, HYBRD, MPSD, ARE, APE, CP, AICc,	Nonlinear	[33]
Compost	Reactive dye	Langmuir, Freundlich, Harkins Jura	R^2, X^2, RMSE	Nonlinear	[47]

Table 6
Models sorted by X^2 statistic from smallest to largest

AB113		AB1		AB80		AR114		AY117	
Model	X^2 P-value diff.	Model	X^2 P-value diff.	Model	X^2 P-value diff.	Model	X^2 P-value diff.	Model	X^2 P-value diff.
Two-Parameter models									
La		La		La		Tem		La	
	3.48E-03		4.23E-01		1.35E-14		0.00E+00		0.00E+00
Tem		Tem		Tem		La		Tem	
	2.62E-02		2.30E-02		8.10E-13		6.44E-15		2.48E-13
Fr		Fr		Jov		Dub		Dub	
	9.22E-06		3.62E-07		2.59E-13		1.38E-13		9.73E-12
Hal		Hal		Dub		Jov		Jov	
	1.90E-01		1.88E-04		1.29E-10		4.90E-13		3.22E-11
Jov		Jov		Fr		Fr		Fr	
	3.25E-01		1.85E-07		2.36E-13		1.33E-15		1.37E-13
Dub		Dub		Hal		Hal		Hal	
	4.55E-01		3.42E-09		2.54E-01		4.08E-06		7.61E-04
Har		Har		Har		Har		Har	
Three-Parameter models									
UN		UN		Vi		Vi		Ra3	
	5.47E-06		2.47E-02		4.00E-15		1.44E-15		0.00E+00
Kob		Kob		Ra1		kh		Fri	
	1.29E-08		7.44E-05		0.00E+00		0.00E+00		0.00E+00
La-Fr		La-Fr		khan		Ra1		Ra2	
	3.95E-06		2.51E-02		3.33E-15		1.22E-15		0.00E+00
Toth		Toth		Ra3		Fri		Jos	
	1.83E-06		1.61E-01		0.00E+00		0.00E+00		0.00E+00
Fri		Ra2		Fri		Ra2		Red	
	1.99E-05		1.49E-04		0.00E+00		0.00E+00		0.00E+00
Red		Fri3		Ra2		Ra3		khan	
	5.11E-10		1.97E-04		0.00E+00		0.00E+00		0.00E+00
Ra2		Red		Jos		Jos		Ra1	
	2.17E-10		1.54E-04		0.00E+00		0.00E+00		8.88E-16
Jos		Jos		Red		Red		Vi	
	1.26E-08		2.48E-04		8.22E-15		5.00E-15		0.00E+00
Ra3		Ra3		Toth		Toth		Toth	
	1.74E-08		2.89E-02		9.99E-16		1.67E-15		0.00E+00
Ra1		Ra1		UN		UN		UN	
	5.58E-06		2.15E-04		2.44E-15		2.55E-15		1.55E-15
Kh		Kh		La-Fr		La-Fr		La-Fr	
	2.16E-09		1.72E-01		0.00E+00		0.00E+00		0.00E+00
Vi		Vi		Kob		Kob		Kob	

La: Langmuir, **Tem**: Temkin, **Fr**: Freundlich, **Hal**: Halsay, **Jov**: Jovanovic, **Dub**: Dubinin-Radushkevich, **Har**: Harkins-Jura, **UN**: UNILAN, **Kob**: Koble-Corrigan, **La-Fr**: Langmuir-Freundlich, **Toth**: Toth, **Fri3**: Three parameter Fritz-Schlunder, **Red**: Redlich- Peterson, **Rad2**: Radke II, **Jos**: Jossens, **Ra3**: Radke III, **Ra1**: Radke I, **Kh**: Khan, **Vi**: Vieth-Sladek

that the local Langmuir equation is applicable on each patch, and the distribution of energy is assumed uniform. The parameter s characterizes the heterogeneity of the surface, the larger the value of this parameter is; the more heterogeneous is the system. The other parameters, the pre-exponential constant, K_u and the monolayer capacity (q_{mu}), are similar to the adsorption parameters of the Langmuir equation. If $s = 0$ the UNILAN equation reduces to the Langmuir isotherm. The parameter s for AB1 and AB113 dyes takes values of 2.037 and 1.644 respectively. These show the heterogeneity of the system.

Table 7
Models sorted by G^2 statistic from smallest to largest

AB113		AB1		AB80		AR114		AY117	
Model	**G2 P-value diff.**	**Model**	**G2 P-value diff.**	**Model**	**G2 P-value diff.**	**Model**	**G2 P-value diff.**	**Model**	**G2 P-value diff.**
Two-Parameter models									
Hal		Tem		La		Dub		La	
	1.11E-05		1.02E-02		3.00E-14		0.00E+00		1.33E-15
La		Hal		Tem		Jov		Dub	
	1.04E-04		5.46E-04		1.54E-12		0.00E+00		7.88E-13
Fr		Fr		Jov		Tem		Tem	
	5.11E-04		1.32E-02		9.00E-13		2.93E-13		8.64E-11
Tem		La		Hal		La		Jov	
	7.80E-01		1.78E-03		8.63E-14		2.46E-12		3.11E-11
Dub		Dub		Fr		Hal		Hal	
	1.51E-01		3.74E-14		2.38E-12		4.33E-14		2.67E-12
Jov		Jov		Dub		Fr		Fr	
	6.54E-02		7.34E-25		3.69E-02		5.70E-05		2.35E-03
Har		Har		Har		Har		Har	
Three-Parameter models									
UN		UN		Vi		Vi		Vi	
	5.68E-06		1.71E-01		3.20E-13		1.88E-12		1.50E-13
Kob		Kob		Ra3		kh		kh	
	1.33E-05		5.51E-03		3.62E-14		6.66E-15		0.00E+00
La-Fr		La-Fr		Ra1		Ra1		Ra1	
	1.34E-05		5.74E-02		1.69E-13		9.43E-13		3.74E-13
Toth		Toth		kh		Fri		Ra3	
	9.47E-05		4.31E-01		4.82E-13		0.00E+00		3.95E-13
Red		Fri		Jos		Ra2		Fri	
	5.72E-06		8.53E-04		0.00E+00		6.62E-14		0.00E+00
Ra2		Ra2		Red		Jos		Ra2	
	1.06E-04		9.33E-04		3.45E-14		0.00E+00		4.44E-15
Fri		Jos		Fri		Red		Jos	
	1.21E-05		2.04E-03		2.89E-15		7.77E-15		0.00E+00
Ra2		Red		Ra2		Ra3		Red	
	4.31E-06		1.16E-03		2.78E-12		2.32E-12		1.03E-11
Ra1		Ra3		Toth		UN		Toth	
	3.58E-05		3.19E-02		9.75E-13		1.61E-12		1.57E-12
khan		kh		UN		Toth		UN	
	2.04E-04		1.33E-03		6.87E-13		3.79E-12		1.20E-11
Jos		Ra1		La-Fr		Kob		La-Fr	
	4.84E-04		1.10E-01		4.22E-14		2.89E-13		1.04E-13
Vi		Vi		Kob		La-Fr		Kob	

La: Langmuir, **Tem**: Temkin, **Fr**: Freundlich, **Hal**: Halsay, **Jov**: Jovanovic, **Dub**: Dubinin-Radushkevich, **Har**: Harkins-Jura, **UN**: UNILAN, **Kob**: Koble-Corrigan, **La-Fr**: Langmuir-Freundlich, **Toth**: Toth, **Fri3**: Three parameter Fritz-Schlunder, **Red**: Redlich-Peterson, **Rad2**: Radke II, **Jos**: Jossens, **Ra3**: Radke III, **Ra1**: Radke I, **Kh**: Khan, **Vi**: Vieth-Sladek

The two-parameter Temkin and three-parameter UNILAN isotherm models were found statistically to be the acceptable models to describe AY117 dye sorption onto GAC F400. With regard to the number of UNILAN parameters and by comparing its statistics with those of other models, UNILAN may be the best fitted model to describe the AY117 adsorption. The UNILAN's s parameter for AY117 dye is 1.709. This shows that the surface of GAC F400 for adsorption of free AY117 may be heterogeneous with a different energy distribution.

The equilibrium sorption data of AR114 dye fitted well to Koble–Corrigan equation. This model is valid only when $\beta > 1$ [23]. The corresponding Koble–Corrigan parameters are given in Table 4. The constant β for the sorption of all the studied dyes is less than unity, meaning that the model is unable to describe the experimental data. Thus for the case of

Table 8
Mann–Whitney U test results

Distribution	N	Mean Rank	Sum Rank	U	Z	Prob > |U| *
Three parameters						
X^2 P-value diff.	55	46.6	2563	1023	−2.94514	0.00323
G^2 P-value diff.	55	64.4	3542			
Two parameters						
X^2 P-value diff.	30	31.1	933.5	468.5	0.26616	0.79012
G^2 P-value diff.	30	29.8	896.5			

* Null Hypothesis: X^2 P-value diff. = G^2 P-value diff., Alternative hypothesis: X^2 P-value difference <> G^2 P-value difference.

AR114 dye, based on G^2, the second best model, that is Langmuir–Freundlich, was chosen as the best descriptive model.

The Langmuir–Freundlich equation has the combined form of Langmuir and Freundlich equations. At low adsorbate concentrations, it reduces to Freundlich isotherm; while at high concentrations, it predicts a monolayer adsorption capacity characteristic of the Langmuir isotherm [24].

The parameter K_{LF} in the Langmuir–Freundlich model is equilibrium constant for a heterogeneous solid, and m_{LF} is the heterogeneity parameter, lies between 0 and 1. The larger is this parameter, the higher is the degree of homogeneity. However, this information does not point to what is the source of homogeneity, whether it can be the GAC F400 structural or energetic properties or the dye property. The parameter m_{LF} for AB80 sorption is 0.994 which is near to unity, suggesting some degree of homogeneity of this dye/activated carbon system. The Langmuir–Freundlich isotherm exhibits the best fit for AR114 adsorption process. The m_{LF} for AR114 adsorption onto GAC F400 is 0.797 and unlike to AB80/GAC F400 system, indicate that the adsorption process is heterogeneous. The adsorption isotherm with the Langmuir–Freundlich model is presented in Fig. 3. As shown in Table 4 Langmuir–Freundlich model describes the adsorption of AB80 and AR114 acceptably. The values of maximum adsorption capacity determined using Langmuir–Freundlich model for AB80 and AR114 are 174.87 and 113.86 mg g^{-1}, respectively. These values are comparable to the experimental adsorption isotherm plateau, which are acceptable.

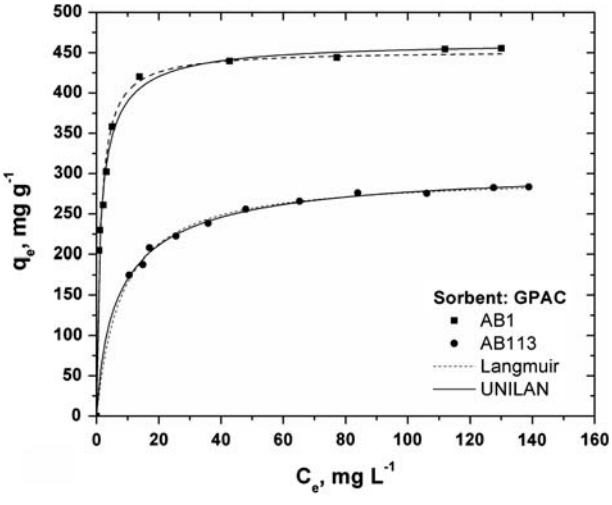

Fig. 2. Experimental points and the best model curves for the adsorption of AB1 and AB113 dyes onto GPAC.

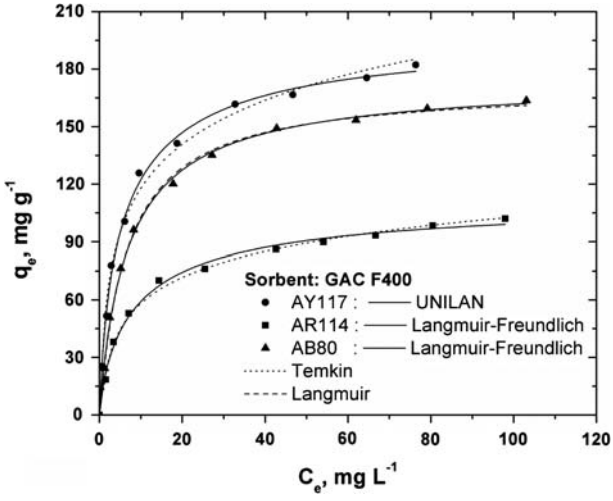

Fig. 3. Experimental and the best model curves for the adsorption of AY117, AR114, and AB80 dyes onto GAC F400.

4. Conclusion

The adsorption equilibrium isotherms of five dyes (Acid blue 113, Acid Black 1, Acid Blue 80, Acid Red 114, and Acid Yellow 117), from aqueous solution onto activated carbon were studied and modeled. A trial-and-error nonlinear method of seven

two-parameter and 12 three-parameter isotherm models was used to determine the best-fit isotherm. The abilities of two well-known G^2 and X^2 statistics to finding the best isotherm model were compared. The sensitivity of G^2 statistic was more than that for X^2 to find the best three-parameter model regarding goodness-of-fit. On the other hand, the X^2 statistic may be more appropriate than G^2 for comparing the models with two parameters. Based on G^2 statistic adsorption isotherm data of AB1 and AB113 dyes onto GPAC indicated a good-fit to the UNILAN three-parameter isotherm model and the sorption processes were heterogeneous. The UNILAN model also found as the best fitted model to describe the AY117 adsorption onto GAC F400. Langmuir–Freundlich model described the adsorption of AR114 and AB80 onto GAC F400 acceptably. The adsorption process for AR114 and AB80 was found heterogeneous and homogeneous, respectively.

Acknowledgments

The authors thank the Hamadan University of Medical Sciences for financial support. The corresponding author would like to thank Prof. Gordon McKay for the provision of some experimental data. Furthermore, thanks to Mr. Siavash Mirzaee Ramhormozi, M.Sc. student of biostatistics from Hamadan University of Medical Science for some suggestions to improve the manuscript.

Nomenclature

- C_e — the equilibrium liquid-phase concentration of the adsorbate ($mg\,L^{-1}$)
- q_e — the equilibrium adsorbate loading onto the adsorbent ($mg\,g^{-1}$)
- C_0 — initial dye concentration ($mg\,L^{-1}$)
- m — sorbent mass (g)
- V — The solution volume (L)
- A_R — the Redlich–Peterson and isotherm constant ($L\,g^{-1}$)
- B_R — the Redlich–Peterson constant having unit of ($L\,mg^{-1}$)
- A_C — the K-C constant ($L^{\beta}\,mg^{1-\beta}\,g^{-1}$)
- B_C — the K-C constant having unit of $(L\,mg^{-1})^{\beta}$
- q_{mLF} — the Langmuir–Freundlich maximum adsorption capacity ($mg\,g^{-1}$)
- K_{LF} — the Langmuir–Freundlich equilibrium constant for a heterogeneous solid
- m_{LF} — the Langmuir–Freundlich heterogeneity parameter, lies between 0 and 1
- q_{mFS} — the Fritz–Schlunder maximum adsorption capacity ($mg\,g^{-1}$)
- K_{FS} — the Fritz–Schlunder equilibrium constant ($L\,mg^{-1}$)
- m_{FS} — the Fritz–Schlunder model exponent
- q_{mRP} — the Radke–Prausnitz maximum adsorption capacities ($mg\,g^{-1}$)
- K_{RP} — the Radke–Prausnitz equilibrium constants
- m_{RP} — the Radke–Prausnitz model exponents
- q_{mT} — the Toth maximum adsorption capacity ($mg\,g^{-1}$)
- K_T — the Toth equilibrium constant
- m_T — the Toth model exponent
- q_{mk} — maximum adsorption capacity in the Khan model ($mg\,g^{-1}$)
- b_k — the Khan constant ($L\,mg^{-1}$)
- β — the Jossens, Koble-Corrigan, Khan, Redlich-Peterson models exponent
- K_u — the UNILAN constant ($L\,mg^{-1}$)
- q_{mu} — maximum adsorption capacity in UNILAN model ($mg\,g^{-1}$)
- s — the UNILAN model constant
- k_j — the Jossens constant ($L\,g^{-1}$)
- j — the Jossens constant having unit of ($L\,mg^{-1}$)
- S_{max} — maximum adsorption capacity in the Vieth–Sladek model ($mg\,g^{-1}$)
- k_L — the Vieth–Sladek constant ($L\,mg^{-1}$)
- k_d — the parameters of the Vieth–Sladek model
- q_m — maximum adsorption capacity in Langmuir model ($mg\,g^{-1}$)
- b — the Langmuir constant related to the energy of adsorption ($L\,mg^{-1}$)
- n — the Freundlich and Halsey equation exponents
- K_f — the Freundlich constant ($mg^{1-1/n}\,L^{1/n}\,g^{-1}$)
- R — universal gas constant ($kJ\,mol^{-1}\,K^{-1}$)
- T — temperature (K)
- b_T — the Temkin constant related to heat of sorption ($kJ\,mol^{-1}$)
- K_{Te} — the Temkin equilibrium isotherm constant ($L\,g^{-1}$)
- K_J — the Jovanovic isotherm constant ($L\,g^{-1}$)
- q_{max} — maximum adsorption capacity in Jovanovic model ($mg\,g^{-1}$)
- Q_s — monolayer saturation capacity in Dubinin–Radushkevich model ($mg\,g^{-1}$)
- B_D — Dubinin–Radushkevich model constant ($mol^2\,kJ^{-2}$)
- ε — Polanyi potential
- A_H — the Harkins–Jura isotherm parameter
- B_H — the Harkins–Jura isotherm constant
- K_H — the Halsey isotherm constant
- N — number of experimental points

References

[1] D. Do Duong, Adsorption analysis: equilibria and kinetics, In: R.T. Yang (Ed), Series on Chemical Engineering, vol. 2, Imperial College Press, London, 1998.

[2] V. Inglezakis, S. Poulopoulos, Adsorption, Ion Exchange and Catalysis: Design of Operations and Environmental Applications, first ed., Elsevier Science, Oxford, 2006.
[3] Y.S. Ho, J.F. Porter, G. McKay, Equilibrium isotherm studies for the sorption of divalent metal ions onto peat: copper, nickel and lead single component systems, Water Air Soil Poll. 141 (2002) 1–33.
[4] D.A. Ratkowsky, Handbook of Nonlinear Regression Models, Marcel Dekker Inc., New York, NY, 1990.
[5] D. Ringot, B. Lerzy, K. Chaplain, J.P. Bonhoure, E. Auclair, Y. Larondelle, In vitro biosorption of ochratoxin A on the yeast industry by-products: comparison of isotherm models, Bioresour. Technol. 98 (2007) 1812–1821.
[6] Y.S. Ho, W.T. Chiu, C.W. Chung, Regression analysis for the sorption isotherms of basic dyes on sugarcane dust, Bioresour. Technol. 96 (2005) 1285–1291.
[7] S. Allen, Q. Gan, R. Matthews, P. Johnson, Comparison of optimised isotherm models for basic dye adsorption by Kudzu, Bioresour. Technol. 88 (2003) 143–152.
[8] Y.S. Ho, Selection of optimum sorption isotherm, Carbon 42 (2004) 2113–2130.
[9] M.C. Ncibi, Applicability of some statistical tools to predict optimum adsorption isotherm after linear and non-linear regression analysis, J. Hazard. Mater. 153 (2008) 207–212.
[10] J.C.Y. Ng, W.H. Cheung, G. McKay, Equilibrium studies for the sorption of lead from effluents using chitosan, Chemosphere 52 (2003) 1021–1030.
[11] A. Malek, S. Farooq, Comparison of isotherm models for hydrocarbon adsorption on activated carbon, A.I.Ch.E.J. 42 (1996) 431–441.
[12] A. Seidel, D. Gelbin, On applying the ideal adsorbed solution theory to multicomponent adsorption equilibria of dissolved organic components on activated carbon, Chem. Eng. Sci. 43 (1988) 79–89.
[13] A. Seidel-Morgenstern, G. Guichon, Modelling of the competitive isotherms and the chromatographic separation of two enantiomers, Chem. Eng. Sci. 48 (1993) 2787–2797.
[14] H. Chernoff, E.L. Lehmann, The use of maximum likelihood estimates in χ^2 tests for goodness-of-fit, Annal. Math. Stat. 25 (1954) 579–586.
[15] J.H. McDonald, Handbook of Biological Statistics, Sparky House Publishing, Baltimore, MD, 2008.
[16] I. Langmuir, The adsorption of gases on plane surfaces of glass, mica, and platinum, J. Am. Chem. Soc. 40 (1918) 1361–1403.
[17] H.Z. Freundlich, Over the adsorption in solution, J. Phys. Chem. 57A (1906) 385–470.
[18] M.M. Dubinin, L.V. Radushkevich, The equation of the characteristic curve of activated charcoal, Dokl. Akad. Nauk SSSR 55 (1947) 327–329.
[19] D.S. Jovanovic, Physical adsorption of gases I: isotherms for monolayer and multilayer adsorption, Colloid Polym. Sci. 235 (1969) 1203–1214.
[20] W.D. Harkins, E.J. Jura, The decrease of free surface energy as a basis for the development of equations for adsorption isotherms; and the existance of two condensed phases in films on solids, J. Chem. Phys. 12 (1944) 112–113.
[21] M. Tempkin, J.V. Pyzhev, Kinetics of ammonia synthesis on promoted iron catalysts, Acta Physiochim. URSS 12 (1940) 217–222.
[22] G. Halsey, Physical adsorption on nonuniform surfaces, J. Chem. Phys. 16 (1948) 931–937.
[23] R.A. Koble, T.E. Corrigan, Adsorption isotherms for pure hydrocarbons, Ind. Eng. Chem. 44 (1952) 383–387.
[24] R. Sips, On the structure of a catalyst surface, J. Chem. Phys. 16 (1948) 490–495.
[25] J. Tóth, Calculation of the BET compatible surface area from any type I. Isotherms measured below the critical temperature, J. Colloid Interface Sci. 225 (2000) 378–383.
[26] O. Redlich, D.L. Peterson, A useful adsorption isotherm, J. Phys. Chem. 63 (1959) 1024–1026.
[27] W. Fritz, E.U. Schlunder, Simultaneous adsorption equilibria of organic solutes in dilute aqueous solution on activated carbon, Chem. Eng. Sci. 29 (1974) 1279–1282.
[28] C.J. Radke, J.M. Prausnitz, Adsorption of organic solutions from dilute aqueous solution on activated carbon, Ind. Eng. Chem. Fund. 11 (1972) 445–451.
[29] L. Jossens, J.M. Prausnitz, Thermodynamics of multi-solute adsorption from dilute aqueous solutions, Chem. Eng. Sci. 33 (1978) 1097–1106.
[30] A.R. Khan, I.R. Al-Waheab, A. Al-Haddad, A generalized equation for adsorption isotherms for multi-component organic pollutants in dilute aqueous solution, Environ. Technol. 17 (1996) 13–23.
[31] J.M. Honig, L.H. Reyerson, Adsorption of nitrogen, oxygen, and argon on rutile at low temperatures; applicability of the concept of surface heterogeneity, J. Phys. Chem. 56 (1952) 140–144.
[32] W.R. Vieth, K.J. Sladek, A model for diffusion in a glassy polymer, J. Colloid Interface Sci. 20 (1965) 1014–1033.
[33] M. Hadi, M.R. Samarghandi, G. McKay, Equilibrium two-parameter isotherms of acid dyes sorption by activated carbons: Study of residual errors, Chem. Eng. J. 160 (2010) 408–416.
[34] M. Hadi, M.R. Samarghandi, G. McKay, Simplified fixed bed design models for the adsorption of acid dyes on novel pine cone derived activated carbon, Water Air Soil Pollut. 218 (2011) 197–212.
[35] K.K.H. Choy, J.P. Porter, G. McKay, Single and multicomponent equilibrium studies for the adsorption of acidic dyes on carbon from effluents, Langmuir 20 (2004) 9646–9656.
[36] ASTM D4607–94, Standard Test Method for Determination of Iodine Number of Activated Carbon, 1999.
[37] A. Agresti, An Introduction to Categorical Data Analysis, 2 ed., John Wiley & Sons, Hoboken, NJ, 2007.
[38] M. Belhachemi, F. Addoun, Adsorption of congo red onto activated carbons having different surface properties: studies of kinetics and adsorption equilibrium, Desalin. Water Treat. 37 (2012) 122–129.
[39] V.S. Mane, I.D. Mall, V.C. Srivastava, Kinetic and equilibrium isotherm studies for the adsorptive removal of Brilliant Green dye from aqueous solution by rice husk ash, J. Environ. Manage. 84 (2007) 390–400.
[40] K.V. Kumar, K. Porkodi, F. Rocha, Isotherms and thermodynamics by linear and non-linear regression analysis for the sorption of methylene blue onto activated carbon: comparison of various error functions, J. Hazard. Mater. 151 (2008) 794–804.
[41] M.C. Shih, Kinetics of the batch adsorption of methylene blue from aqueous solutions onto rice husk: effect of acid-modified process and dye concentration, Desalin. Water Treat. 37 (2012) 200–214.
[42] H. Zhu, M. Zhang, Y. Liu, L. Zhang, R. Han, Study of congo red adsorption onto chitosan coated magnetic iron oxide in batch mode, Desalin. Water Treat. 37 (2012) 46–54.
[43] J. Liang, J. Wu, P. Li, X. Wang, B. Yang, Shaddock peel as a novel low-cost adsorbent for removal of methylene blue from dye wastewater, Desalin. Water Treat. 39 (2012) 1–6.
[44] L. Zhang, S. Hong, J. He, F. Gan, Y.S. Ho, Adsorption characteristic studies of phosphorus onto laterite, Desalin. Water Treat. 25 (2011) 98–105.
[45] M. Matheswaran, Kinetic studies and equilibrium isotherm analyses for the adsorption of methyl orange by coal fly ash from aqueous solution, Desalin. Water Treat. 29 (2011) 241–251.
[46] M.R. Samarghandi, M. Hadi, S. Moayedi, F. Barjasteh Askari, Two-parameter isotherms of methyl orange sorption by pinecone derived activated carbon, Iran J. Environ. Health Sci. Eng. 6 (2009) 285–294.
[47] G. McKay, M. Hadi, M.T. Samadi, A.R. Rahmani, M. Solaimany Aminabad, F. Nazemi, Adsorption of reactive dye from aqueous solutions by compost, Desalin. Water Treat. 28 (2011) 1–10.